Marine Geology, 71 (1986) 237—258
Elsevier Science Publishers B.V., Amsterdam — Printed in The Netherlands

SUSPENDED SEDIMENT TRANSPORT IN AN ESTUARINE TIDAL CHANNEL WITHIN SAN FRANCISCO BAY, CALIFORNIA

R.W. STERNBERG[1], D.A. CACCHIONE[2], D.E. DRAKE[2] and KATE KRANCK[3]

[1]*School of Oceanography, University of Washington, Seattle, WA 98195 (U.S.A.)*
[2]*U.S. Geological Survey, 345 Middlefield Road, Menlo Park, CA 94025 (U.S.A.)*
[3]*Bedford Institute of Oceanography, Dartmouth, N.S. B2Y 4A2 (Canada)*

(Received March 4, 1985; revised and accepted August 18, 1985)

ABSTRACT

Sternberg, R.W., Cacchione, D.A., Drake, D.E. and Kranck, K., 1986. Suspended sediment transport in an estuarine tidal channel within San Francisco Bay, California. Mar. Geol., 71: 237—258.

A recently developed instrumentation system has been used to monitor simultaneously flow conditions and suspended sediment distribution in the bottom boundary layer of a tidal channel within San Francisco Bay, California. Measurements were made every 15 min over six successive flood and ebb tidal cycles. They included mean velocity profiles from four electromagnetic current meters within 1 m of the seabed; mean suspended sediment concentration profiles from seven miniature nephelometers placed within 1 m of the seabed; near-bottom pressure fluctuations; vertical temperature gradient; and bottom photographs. Additionally, suspended sediment was sampled from four levels within 1 m of the seabed three times during the tidal cycle. The instrument system was retrieved during each slack water period to exchange suspended sediment sample bags. While the instrument was deployed STD-nephelometer measurements were made thoughout the water column and water samples were collected each 1—2 h and bottom sediment was sampled at the deployment site.

Size distributions of the suspended sediment samples, estimates of particle settling velocity (w_s), friction velocity (U_*), and reference concentration (C_a) at z = 20 cm were used in the suspended sediment distribution equations to evaluate their ability to predict the observed suspended sediment profiles. Three suspended sediment particle conditions were evaluated: (1) individual particle sizes in the 4—11 ϕ (62.5—0.5 μm) size range with the reference concentration C_a at z = 20 cm (C_ϕ); (2) individual particle sizes in the 4—6 ϕ size range, flocs representing the 7—11 ϕ size range with the reference concentration C_a at z = 20 cm (C_f); and (3) individual particle sizes in the 4—6 ϕ size range, flocs representing the 7—11 ϕ size range with the reference concentration predicted as a function of the bed sediment size distribution and the square of the excess shear stress. An analysis was also carried out on the sensitivity of the suspended sediment distribution equation to deviations in the primary variables w_s, U_*, and C_a. In addition, computations of mass flux were made in order to show vertical variations in mass flux for varying flow conditions.

INTRODUCTION

The erosion of fine bottom sediment and its transport as suspended load is an important aspect of sedimentation in the shallow-marine environment.

0025-3227/86/$03.50

Many observations have shown that inorganic particulates introduced into the coastal environment undergo numerous cycles of erosion and deposition before reaching a permanent depositional site. This cyclic transport phenomenon is best exemplified in the estuarine environment and is also prominent as a dispersal mode on continental shelves; in fact, it occurs in any environment where boundary shear stresses exceed sediment threshold conditions on a frequent or periodic (e.g., seasonal) basis.

Mathematical expressions to describe or predict quantitatively the distribution of suspended sediment and associated particle flux in open channel flow were derived in the 1930's and have been applied extensively by marine scientists. It is noteworthy, however, that suspended sediment distribution equations have not been well tested in the sea, and thus marine scientists using these relationships have no perspective on the precision or even the applicability of their results. As recently as 1981 Adams and Weatherly state that "the virtual absence of contemporaneous flow and suspended-sediment measurements mandates a modeling approach to this problem".

This paper reports the initial results of a continuing field investigation of suspended sediment dynamics in the shallow-marine environment. The primary objective is to test the applicability of various suspended sediment distribution equations under flow conditions where resuspension of bottom sediment occurs and significant quantities of sediment are being transported. An area characterized by strong tidal currents and fine bottom sediments in San Francisco Bay, California, was selected for the study. A combination of new and existing instrumentation was used in an attempt to measure all of the flow and suspended sediment variables required to test several suspended sediment distribution equations. The resulting data set is unique; it provides a detailed view of the temporal and spatial characteristics of the suspended sediment field within 1 m of the seabed and concurrent observations of flow conditions.

BACKGROUND

A general hypothesis to physically explain the vertical distribution of suspended sediment in a homogeneous boundary layer flow was introduced by Rouse (1937) and has been applied extensively by oceanographers over the past several decades (Komar, 1978). The mathematical treatment is based on a steady-state balance of upward turbulent diffusion and gravitational settling by particles by the relation:

$$\frac{C}{C_a} = \left(\frac{h-z}{z} \cdot \frac{a}{h-a}\right)^{\frac{w_s}{kU_*}} \tag{1}$$

where C is the sediment concentration of the rth size class at distance z off the bottom, C_a is a reference concentration for that size class at distance a, h is the total depth, w_s is particle settling velocity, k is Von Karman's constant, U_* = friction velocity = $(\tau_0/\rho)^{1/2}$ where τ_0 is the boundary shear stress and ρ is fluid density (Task Committee, 1963).

Equation (1) is called the suspended load distribution equation or sometimes the Rouse equation (Task Committee, 1963). This particular form was derived with the assumptions that the eddy viscosity for momentum (K_m) = $kU_*z(h-z)/h$ and that the eddy viscosity for sediment (K_s) is equal to that of momentum (K_m). In practice, a reference level concentration (C_a) must be obtained and eqn.(1) is solved for either a bulk sediment sample or for each size class when more than one size class is in suspension.

Several techniques have been suggested or employed to adjust the parameters in eqn.(1) to reflect marine boundary layer mechanics and the influence of suspended sediment on flow conditions. Some examples are: Empirical adjustments of Von Karman's constant (e.g., Einstein and Chien, 1952, 1955; Vanoni, 1953; McCave, 1973), nonlinear approximations to the eddy viscosity profile (e.g., Smith and McLean, 1977; Vincent et al., 1982), and a Richardson number correction for sediment-induced stratification. Empirical adjustments to k and K_s have not been considered in this study; however, adjustments based on sediment-induced stratification as expressed by a Richardson number have been made. The use of a Richardson number to adjust the basic sediment transport equations to account for sediment-induced stratification has been considered by many scientists (e.g., Sundborg, 1956; Smith and McLean, 1977; Heathershaw, 1979; Adams and Weatherly, 1981). A simplified form of this correction, assuming a constant value of the flux Richardson number (R_f) in the lower boundary layer (Adams and Weatherly, 1981), is expressed as a modification to the Karman-Prandtl equation:

$$\overline{U}_z = \frac{U_*}{k'} \ln\left(\frac{z}{z_0}\right) \tag{2}$$

where $\overline{U}_z$ is the mean velocity at z, U_* is the friction velocity, z_0 is the roughness length, and $k' = k/(1 + 5.5\,R_f)$, where k is Von Karman's constant, and R_f is the flux Richardson number. Smith and McLean (1977) use a gradient Richardson number (Ri) to correct for sediment-induced stratification:

$$Ri = \left[\frac{-(\rho_s - \rho)g}{\rho} \cdot \frac{\partial C_T}{\partial z}\right]\left(\frac{\partial u}{\partial z}\right)^{-2} \tag{3}$$

where ρ_s and ρ are sediment and fluid densities, respectively, g is the acceleration of gravity, $\partial C_T/\partial z$ and $\partial u/\partial z$ are the vertical gradients of total suspended sediment concentration and velocity, respectively. The term $\partial u/\partial z$ can be approximated by U_*/kz for steady flow as described by the Karman-Prandtl equation. The flux and gradient Richardson numbers are related by the ratio of the eddy diffusivity of mass and momentum (i.e., $R_f = K_s/K_m\ Ri$), thus with the assumption that $K_s \sim K_m$ [as used in eqn. (1)], $R_f \sim Ri$.

Another modification of eqn.(1) involves the estimation of the reference concentration (C_a) from bottom sediment texture and flow conditions. Previous efforts to predict reference concentrations include studies of river

and flume conditions (Lane and Kalinski, 1939; Pien, 1941; Hsia, 1943) and modeling of marine boundary layers (Smith, 1977; Smith and McLean, 1977; Adams and Weatherly, 1981; Wiberg and Smith, 1983; Glenn, 1983; Shi et al., 1985; Kachel and Smith, in press; Drake and Cacchione, in press).

The general relationship as applied by the investigators studying marine boundary layers is:

$$C_a = \frac{\gamma_0 i_b C_b S}{1 + \gamma_0 S} \tag{4}$$

where C_a is the volume concentration of a size class at a reference level a (frequently chosen at level z_0 and often approximated as 1 cm), i_b is the proportion of a phi size in the bed sediment, C_b is the bed volume concentration [(1 — porosity) or approximately 0.65], γ_0 is an empirical constant determined to be 2.4×10^{-3} by Smith and McLean (1977), 1.6×10^{-5} by Wiberg and Smith (1983), or a range of 2×10^{-5}—5×10^{-4} by Drake and Cacchione (in press), and S is the excess shear stress = $(\tau_0 - \tau_c)/\tau_c$ where τ_0 is boundary shear stress and τ_c is the critical shear stress. Shi et al. (1985) present a square-root relationship for the term on the right-hand side of eqn.(4) for wave—current environments of the continental shelves of Washington and the Beaufort Sea. These formulations have the advantage of providing a value of C_a for eqn.(1) without requiring measurement of a reference concentration.

INSTRUMENTATION

For this study the instrumented tripod system GEOPROBE was fitted with a multiple nephelometer-suspended sediment sampling system. GEOPROBE is designed to operate on the seafloor for periods of up to three months and to depths of 300 m (Cacchione and Drake, 1979). The tripod platform contains: (1) Marsh McBirney electromagnetic current meters mounted in a vertical array at distances of 20, 50, 70 and 100 cm above the seafloor; (2) a Savonius rotor/vane current meter located at z = 1.5 m; (3) a Paroscientific pressure sensor at z = 2 m; (4) a transmissometer at z = 2 m; (5) a Benthos 35 mm stereo camera and strobe system at z = 1.5 m; (6) two temperature sensors at z = 150 and 35 cm; (7) a digital compass; (8) a Sea Data Corporation Electronics unit that controls the sampling sequence and data recording.

The suspended sediment monitoring and sampling system mounted on the GEOPROBE tripod includes eight miniature nephelometers located on a structural rod within 1 m of the seabed and suspended sediment sampling nozzles mounted in a vertical array at z = 20, 50, 70 and 100 cm. The four sampling nozzles are connected to pumps and to twelve 2 l sample bags located in the upper area of GEOPROBE so that three suspended sediment profiles can be collected during a sampling period. The sampling sequence of the nephelometers and the suspended sediment samplers is synchronized with the operation of GEOPROBE so that boundary layer fluid and flow

conditions and suspended sediment concentration profiles are monitored on a continuous basis and suspended sediment profiles are sampled on a limited basis during each deployment period. A complete description of this system is given in Sternberg et al. (1986).

METHODS

Study site

A tidal channel in San Francisco Bay, east of Southampton Shoal between Richmond and the Tiburon Peninsula, was selected for this study after reconnaissance side-scan and bottom sediment sampling surveys of numerous channels within the bay area. The channel is characterized by strong tidal currents, minimal exposure to surface gravity waves, and a lack of major bedforms (sand waves, etc.). The bottom sediment was dominated by silt (54%) with smaller percentages of clay (34%) and sand (12%) and local sampling revealed relatively uniform textural characteristics both up and down channel. The silt dominance and textural homogeneity at the sampling site were considered to be indicative of minimal sediment cohesive effects and small horizontal concentration gradients. The mean depth at the sampling site was approximately 7 m. Tides are a semidiurnal-mixed type with a diurnal range of 1.8 m. During the experiment (1—3 December 1982) six successive tidal cycles were sampled. The specific location of the GEOPROBE system during each deployment is shown in Fig.1.

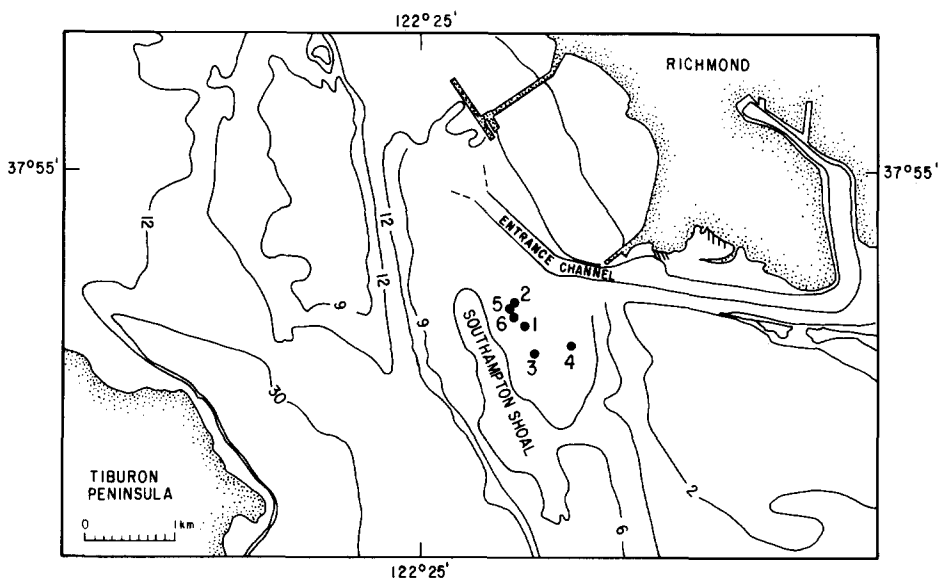

Fig.1. Study site in San Francisco Bay, California, showing the position of the GEOPROBE system deployments (*1—6*).

Sampling procedure

For the field experiments the GEOPROBE system was deployed during successive flood and ebb tidal cycles. GEOPROBE sampling cycles were set at 15 min and during each cycle 7.5 min of 1 s burst measurements of current velocity at z = 20, 50, 70 and 100 cm, pressure at z = 2 m, and temperature at z = 35 and 150 cm were made. During each cycle, the mean velocity at z = 1.5 m was measured and a bottom photograph was taken.

Suspended sediment measurements were made concurrently with the GEOPROBE observations. During each 15 min cycle, output from seven miniature nephelometers, located at z = 14, 20, 30, 49, 52, 70 and 100 cm, were recorded at a 2 Hz rate for a 2 min duration. The 2 Hz sampling rate was dictated by the data logging system. At 30 min, 2 h, and 3.5 h into each tidal cycle, suspended sediment samples were collected at z = 20, 50, 70 and 100 cm. This sequence was varied occasionally during the experiment to sample other times during the tidal cycle. The GEOPROBE system was recovered during each slack water period and sediment sample bags were replaced.

Additional measurements within the water column were made from shipboard while the GEOPROBE system was deployed. These included STD-nephelometer profiles and water samples at 1—3 levels in the water column each 1—2 h. Bottom sediment samples were also collected at the deployment site.

DATA ANALYSES

Flow conditions

The results of the GEOPROBE measurements plotted at 15 min intervals are summarized in Fig.2. The times when suspended sediment profiles were sampled, the sample number, and the periods when the GEOPROBE system was retrieved to replace sediment sampling bags are marked. Tide curves (Fig.2A) show the predicted heights for Golden Gate and Point Richmond adjacent to the study site and are included for reference only. Although mean pressure is measured by GEOPROBE, the deployment station depths vary slightly between each deployment, thus the pressure curve is fragmented and difficult to reconstruct.

The magnitude of U_* was estimated from the slope of the velocity profiles constructed from 7.5 min mean values of the four electromagnetic current meter outputs (Fig.2B). The computational method used for the estimates is given in Cacchione and Drake (1979). During the sampling period the magnitude of U_* varied from 0.08 to 5.2 cm s^{-1}.

The mean speed from the upper electromagnetic current meter ($\overline{U}_{100}$) varied between 0.6 and 76.7 cm s^{-1} over the sampling period (Fig.2C). The flow directions within the channel are ~290° mag during maximum floods and ~70° mag during maximum ebbs.

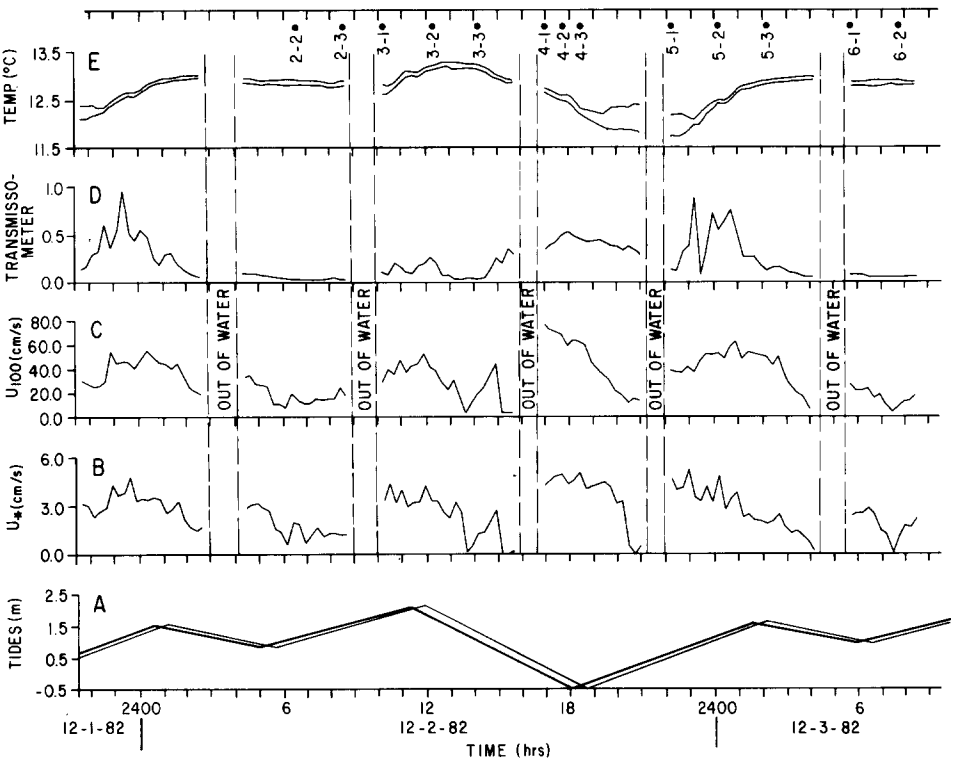

Fig.2. Time series of GEOPROBE output, including (A) the tidal prediction curve for the Golden Gate (heavy line) and Richmond Point (light line); (B) is the friction velocity; (C) is the mean speed at z = 100 cm; (D) is the relative output of the transmissometer at z = 2 m; (E) is the water temperature measured at z = 35 cm (lower curve) and z = 200 cm (upper curve). Times when GEOPROBE was out of the water and when suspended sediment profiles were samples are also shown.

The transmissometer output shown in Fig.2D is for reference only. The vertical scale is in arbitrary units and has not been converted to concentration values.

The water temperature, measured by thermistors located at z = 35 and 150 cm above the seabed, varied between 11.7° and 13.2°C (Fig.2E). Throughout the sampling period the difference between the two temperature sensors was consistently within 0.1°C except at the beginning of the record on 1 December at about 21.30 h and 2 December between 17.30 and 29.30 h when there was a temperature difference of 0.3 and 0.6°C, respectively.

Hydrographic conditions in the water column varied considerably in relation to tidal phase. STD profiles varied from isopycnal during high tide to those showing various degrees of salt wedge intrusion during tidal changes at times of lower—low tides (indicated by the temperature gradients in Fig.2E).

Suspended sediment distribution

All of the nephelometers were calibrated using bottom sediment from the field site placed in a calibration tank. The sensors located at z = 20, ~50, 70, and 100 cm were also calibrated with the in-situ suspended sediment samples collected during the experiment. A calibration curve for one of the OBS sensors which indicates the values from both the laboratory calibration and the in-situ sample results is shown in Fig.3. Although the scatter of the in-situ values is greater than that of the laboratory values, the least-squares analyses of the two are the same.

The time series of suspended sediment concentration within the boundary layer is shown in Fig.4. The times when suspended sediment profiles were sampled, the sample number, and the periods with GEOPROBE was out of water are also indicated. Data logger problems occurred during the first tidal cycle (sampling series no.1) so the data plot begins with the second sampling period. Concentrations vary between 40.1 and 1770 mg l^{-1} at z = 14 cm and 0.7 and 910 mg l^{-1} at z = 100 cm. Although increases in suspended sediment concentration occur during each tidal series, major increases are seen during the fourth and fifth series associated with the time of maximum tidal fluctuations (Fig.2A).

Suspended sediment profiles were plotted for each 15 min cycle throughout the total time series; however, because of the large number of profiles (91), only representative profiles from each tidal series (profiles 2-2, 3-2, 4-2, 5-2, 6-2), and the profile at the time of the highest suspended sediment concentration (2400, 2 December) are shown (Fig.5). In general, the sus-

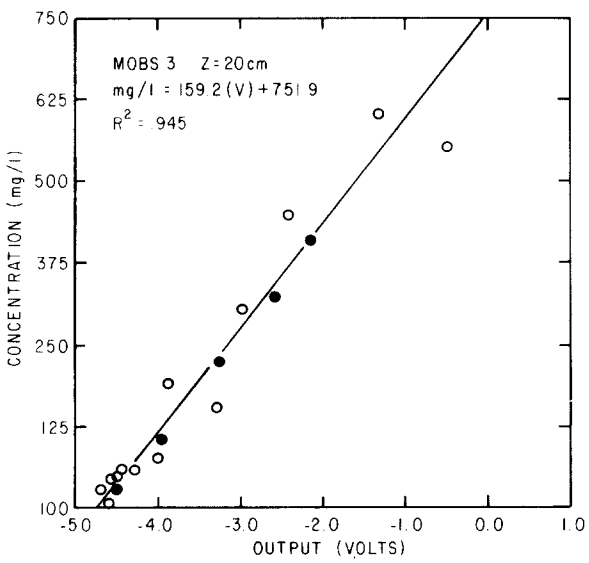

Fig.3. Calibration curve for the nephelometer located at z = 20 cm. Solid circles indicate the laboratory calibration using San Francisco Bay, California, bottom sediment; open circles in-situ samples of suspended sediment.

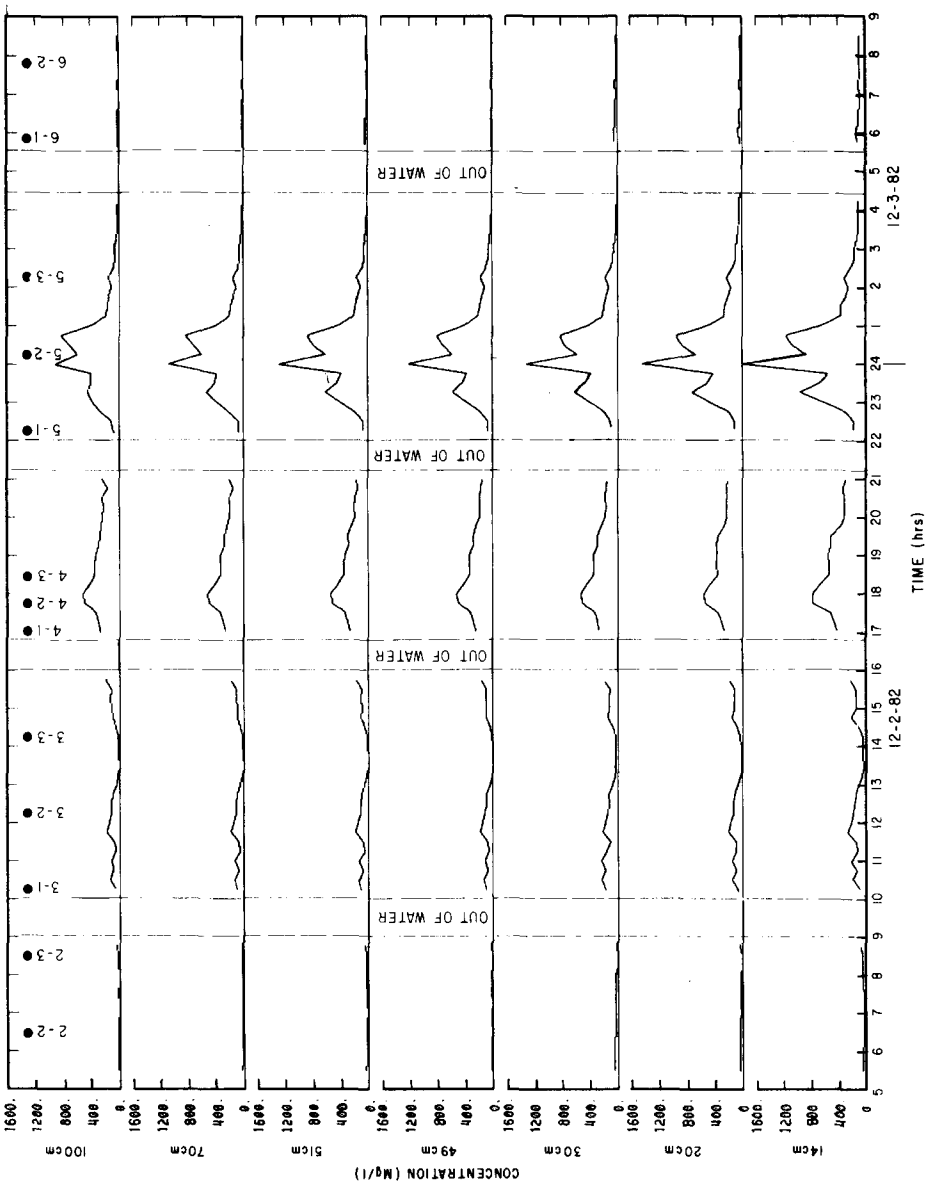

Fig.4. Time series of suspended sediment concentrations from nephelometer outputs located at seven levels above the bed. Times when GEOPROBE was out of the water and when suspended sediment profiles were sampled are also shown.

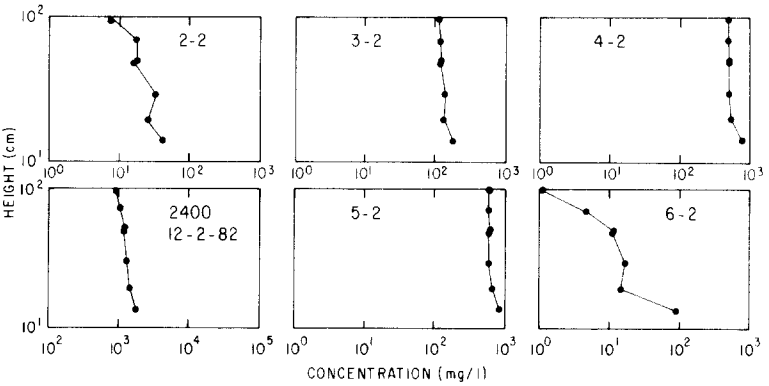

Fig.5. Examples of suspended sediment profiles from nephelometer outputs. Note the scale change for the profile measured at 24.00 h. (See Fig.4 for times when the other profiles were sampled.)

pended sediment concentrations show a systematic decrease away from the boundary with a relatively sharp gradient occurring in the lower part of the profile (e.g., 3-2, 4-2, 6-2).

Suspended sediment texture

Since it is impossible to collect unaltered samples of suspended sediment with a pumping mechanism, analytical procedures were used to uniformly disaggregate all particulates as described by Kranck and Milligan (1979). Size analysis was carried out on all of the suspended sediment samples using a Coulter Counter. The samples were filtered onto Millipore filters in the field. Prior to analyses all filters were eliminated by low-temperature ashing, and the sediment residue treated with hydrogen peroxide, and sonified to ensure that deflocculated single mineral grains were analyzed. Three or four Coulter tubes were used in each analysis to cover the range of particle sizes.

The size spectra are presented as percent frequency distributions of log volume concentration in parts per million versus log diameter in μm. Size analysis is reported in 1/3 ϕ size increments over the range 0.5—200 μm. An example of the size distribution of a suspended sediment profile (profile 4-2) is shown in Fig.6; the four plots are from raw data collected simultaneously at 20, 50, 70, and 100 cm above the seabed.

The nephelometer profiles were obtained every 15 min and appear relatively precise, showing systematic spatial and temporal trends resulting from input from seven sensors whereas the suspended sediment samples represent a much smaller data set with greater scatter (Fig.3). Thus it seems justifiable to adjust the total concentrations of the suspended sediment samples to agree with the corresponding nephelometer outputs. This analytical adjustment was made by converting the nephelometer mass concentration to volume concentration by using a density of 2.3 g cm^{-3}, as suggested

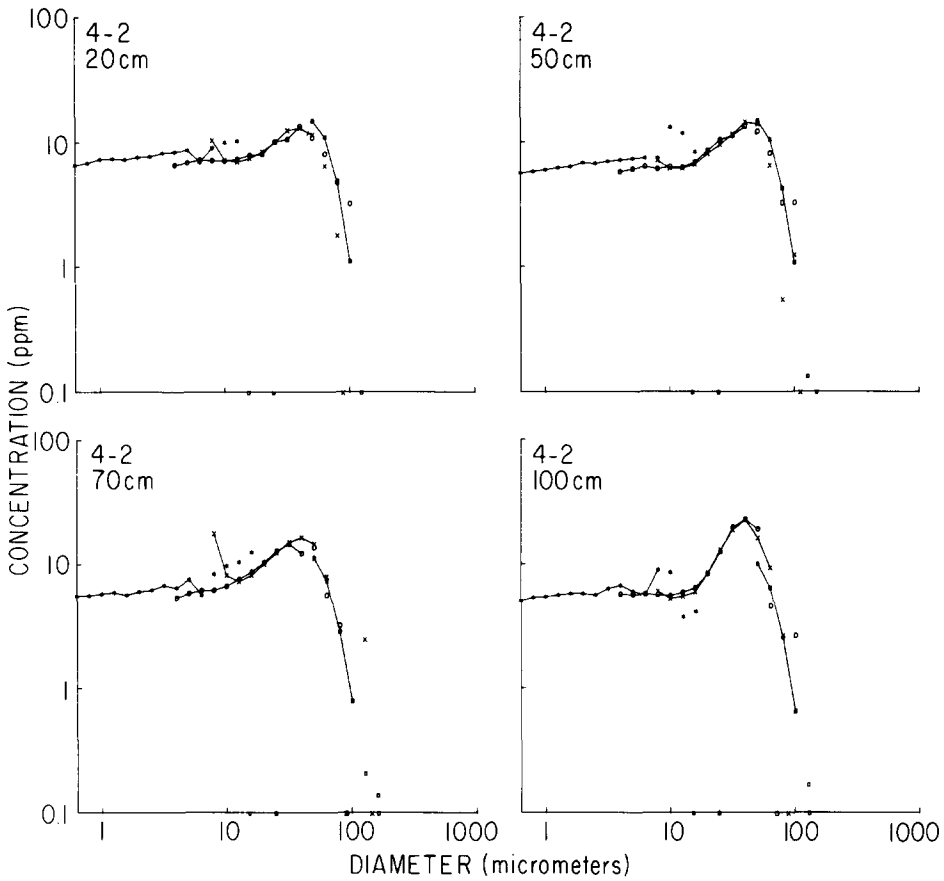

Fig.6. Size distribution of suspended sediment samples from profile 4.2 (see Fig.5). Symbols designate sizes of Coulter Counter tubes used. Data points for each 1/3 ϕ increment are connected if over 50 particles were counted during the analysis. These distributions are from the Coulter Counter outputs and have not been adjusted to equal the total concentration as determined by the miniature nephelometers.

by Kranck and Milligan (1979), and then converting the percent volume for each phi-size in the Coulter Counter analysis by a factor so that the total volume concentration of each suspended sediment sample (in ppm) equals the mass concentration of the equivalent nephelometer output divided by 2.3. Thus the total sample concentration is obtained by the nephelometer output and the size distribution of particles is obtained by Coulter Counter analysis. The results of this comparative adjustment in terms of total sample mass concentrations, volume concentrations, and particle distribution by phi size for all of the suspended sediment samples collected at z = 20 cm are tabulated in Table 1.

Bottom sediment texture

Samples of bottom sediment were collected at the deployment site with a Van Veen grab sampler. The surface centimeter of sediment was sampled

TABLE 1

Summary of basic data set

Profile	Depth h (m)	Friction velocity U_* (cm s^{-1})	Total concentration at z = 20 cm		Particle size distribution									Floc assumption	
			C_{total} (mg l^{-1})	C_{total} (ppm)	3ϕ (ppm)	4ϕ (ppm)	5ϕ (ppm)	6ϕ (ppm)	7ϕ (ppm)	8ϕ (ppm)	9ϕ (ppm)	10ϕ (ppm)	11ϕ (ppm)	$C_{7-11\,\phi}$ (ppm)	w_s (cm s^{-1})
2-2	6.3	2.0	25.8	11.2	0.03	0.1	0.8	1.3	1.7	2.2	2.1	1.9	1.2	9.1	0.33
2-3	5.4	1.2	35.9[b]	15.6	—	0.2	1.2	1.5	2.0	1.9	3.0	3.0	1.8	11.6	0.33
3-1	5.9	3.1	65.6	28.5	—	0.1	3.0	3.3	3.5	5.3	5.5	4.5	2.8	21.6	0.20
3-2	6.5	3.3	130.8	56.9	—	1.0	9.9	8.6	7.7	9.7	8.5	7.1	4.4	37.4	0.15
3-3	5.2	1.3	30.6	13.3	—	0.2	1.4	1.9	2.1	2.3	2.1	2.0	1.3	9.8	0.25
4-1	4.1	4.2	264.6	115.1	—	7.0	24.6	20.2	14.9	15.7	13.3	11.8	7.7	63.3	0.0003
4-2	4.2	5.0	529.0	230.0	0.09	20.6	49.7	31.0	26.2	29.5	28.9	27.0	16.4	128.0	0.07
4-3	4.3	4.7	355.4	154.5	0.09	11.3	46.1	24.7	15.4	16.7	15.4	14.7	10.2	72.4	0.0003
5-1	4.4	4.8	105.4	45.8	—	2.0	5.5	5.1	5.7	7.7	8.0	7.3	4.7	33.3	0.50
5-2	5.8	4.9	664.3	288.8	0.10	4.6	46.8	49.0	39.1	43.0	40.5	37.8	27.8	188.3	0.25
5-3	6.3	3.5	218.5	95.0	—	1.4	13.3	17.8	14.8	15.1	12.7	12.1	7.8	62.5	0.55
6-1	7.3	2.3	38.5	16.8	—	1.5	4.1	2.2	1.9	2.1	2.1	1.8	1.1	9.0	0.45
6-2	8.3	1.1	14.7	6.4	—	0.2	0.8	0.8	0.8	1.2	1.1	1.0	0.6	4.6	0.50
															$\bar{w}_s = 0.28$
Bottom sediment			1.274[c]	553,913	12,740	104,136	142,910	61,484	47,637	54,283	51,514	47,637	31,573	232,643	
i_b					0.023	0.188	0.258	0.111	0.086	0.098	0.093	0.086	0.057	0.420	
w_s (cm s^{-1})					1.37	0.44	0.123	0.030	0.007	0.0014	0.003	0.0001	0.0001	0.28	
τ_c (dyne cm^{-2})					1.21	0.90	0.61	0.49	0.49	0.49	0.49	0.49	0.49	0.49	

[a] From nephelometer output; [b] extrapolation from adjacent data points; and [c] g cm^{-3}.

and subjected to both Coulter Counter analyses, as described above, and to size analyses using sieves for the sand sizes and a hydrophotometer for the fine fractions. The results of the analyses show that the bottom sediment at a central location within the deployment area is composed of 11.8% sand, 54.3% silt, and 33.9% clay. It has a median diameter of 7.06 ϕ (0.0075 mm), mean diameter of 7.61 ϕ, and a sorting coefficient of 2.86 ϕ. The bulk density of the sample was 1.274 g cm^{-3} (volume concentration = 0.554) and the size analysis analyzed by Coulter Counter are summarized in Table 1.

DISCUSSION

Of the 91 suspended sediment profiles measured by the nephelometer array during the field experiment, the 13 profiles measured at the same time that suspended sediment samples were collected (Fig.4) have been chosen for detailed analyses. Thus they have been analyzed for particle size, thereby making it possible to determine reference concentrations (C_a) and settling velocity (w_s) values for each phi size class. The level of the lowest suspended sediment sample (20 cm) is chosen as the reference level (a) and reference concentration (C_a) for each of the 13 profiles (Table 1).

Estimates of settling velocity (w_s) and the critical or threshold value of boundary shear stress (τ_c) for each phi size class have been determined. The value of w_s representing the particle diameter of the middle of the phi size class was chosen as representative for the size class (i.e., 4.5 ϕ diameter to represent the 5 ϕ size class). The settling velocities were selected from Dietrich (1982) for conditions of sediment density of 2.65 g cm^{-3}, fluid density of 1.02 g cm^{-3} and subrounded grains (Corey shape factor of 0.7, and Power's roundness value = 3.5). Values of τ_c for each size class were estimated from existing curves (Miller et al., 1977; Nowell et al., 1981). Estimates of w_s and τ_c for each size class and for U_* computed from the velocity profile analysis, except for one profile, are given in Table 1. The correlation coefficient of the linear regression of the 5-3 velocity profile was very poor so a quadratic relationship $U_*^2 = C_D \overline{U}_{100}^2$ with the value of $C_D = 5.0 \times 10^{-3}$, which was representative of the other profiles during high flow conditions, was used for the U_* estimate.

Particle characteristics

Particle characteristics have a strong bearing on selecting w_s and τ_c values to represent the fine fraction. For example, the presence or absence of flocculated sediment would significantly alter w_s and possibly τ_c. Although direct data were not obtained to determine the in-situ particle characteristics, analyses of the particle-size distributions of the suspended load in relation to the bed sediment suggest that particles in the 7—11 ϕ range may occur as flocs (Table 1).

This speculation is based on a comparison of the relative size distributions of samples of suspended sediment at z = 20 cm and of bottom sediment

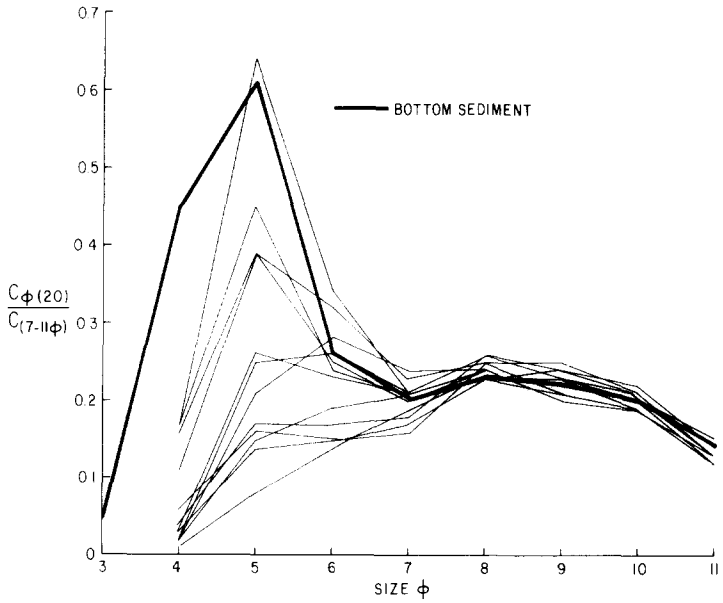

Fig.7. Ratio of sediment concentration by ϕ size and total concentration of the 7—11 ϕ size range cs. ϕ size. (The 3—11 ϕ size range corresponds to 125—0.5 μm particle diameters). Thin lines indicate suspended sediment concentrations at z = 20 cm; the bold line indicates bottom sediment.

(Fig.7). The 3 ϕ size is not included because the particle counts in the Coulter Counter analysis of the suspended sediment samples were generally too low to obtain statistically valid concentrations. The size distributions have been normalized by the concentration of 7—11 ϕ sizes, thus the curves illustrate shape similarities and not total concentrations. The superimposed spectra show that the shapes of the particle-size distribution in the 7—11 ϕ range are virtually the same for all reference samples and for the bed sediment as well. The coarser particles (4—6 ϕ) tend to have a different distribution for each profile, i.e., they react individually to variations in boundary shear stress (Fig.7). The 7—11 ϕ particles maintain their relative distribution regardless of total concentration or the magnitude of the boundary shear stress, suggesting that the assemblage of particles in this size range occurs as aggregates and that the number of aggregates changes away from the bed but not the relative size distribution. The observation that relative grain-size distributions remain constant when the total concentration changes has been reported by Kranck (1980) and Kranck and Milligan (1980). For the above reason a parallel line of analyses has been carried out using the assumption that the 7—11 ϕ particles occur as flocs; a representative value of w_s = 0.28 cm s^{-1} was selected (the method will be discussed below). This value is within the range observed in estuaries (e.g., Krone, 1972) or for flows produced under controlled conditions (Kranck and Milligan, 1980).

Reference concentration

Equation (4) has been used as a guideline to predict the reference concentration (C_a) from the bed concentration ($i_b C_b$) and excess shear stress [$S = (\tau_0 - \tau_c)/\tau_c$]. The value of τ_c for the threshold value of the flocculated sediment was selected from the time series of U_* (Fig.2B) and C (Fig.4; z = 20 cm). At 13.40 h on 2 December the value of U_* was well below threshold (0.15 cm s^{-1}), and the suspended sediment concentration was also low. At 14.00 h, the suspended sediment concentration began to increase slightly and the corresponding value of U_* was approximately 0.7 cm s^{-1} (τ_c = 0.49 dynes cm^{-2}).

Since the denominator $(1 + \gamma_0 S)$ in eqn.(4) is numerically very close to 1*, then eqn.(4) reduces to:

$$\frac{C_a}{i_b C_b} \alpha S \tag{5}$$

which is used to compare the normalized reference concentration and excess shear stress (Fig.8A). Data points for 4—6 ϕ particles and flocs representing the 7—11 ϕ size range are plotted. The data for suspended sediment profile 5-1 has been omitted because the large temperature gradient occurring at that time represents non-neutral buoyancy conditions and is associated with significantly reduced suspended load. Figure 8A shows a nonlinear relationship between $C_a/i_b C_b$ and S. A linear fit is obtained with respect to S^2 as illustrated in Fig.8B. The linear regression for these data is:

$$\frac{C_a}{i_b C_b} = 2.53 \times 10^{-7} S^2 + 3.63 \times 10^{-6} \tag{6}$$

with R^2 = 0.875.

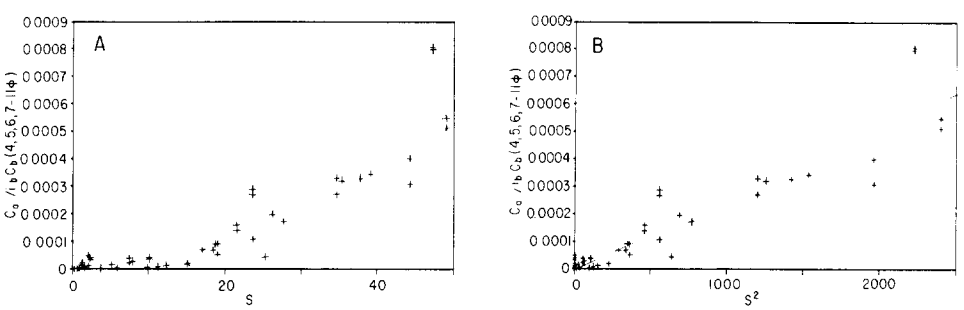

Fig.8. Ratio of the concentrations of suspended sediment in the 4, 5, 6, and 7—11 ϕ size classes at z = 20 cm to the concentration in the bed sediment vs. (A) excess shear stress and (B) excess shear stress squared.

*For γ_0 = 2.4×10^{-3} (Smith and McLean, 1977) or 1.6×10^{-5} (Wiberg and Smith, 1983) and the upper limit of S approximately equals 50, then $(1 + \gamma_0 S)$ would be 1.12 and 1.0008, respectively.

Equation (6) represents an empirical fit of the data using eqn.(4) as a guideline. The plots shown in Fig.8 include numerous boundary layer sediment effects (e.g., sediment-induced stratification at high values of S and sediment armoring) that are considered independently from the computation of C_a in the numerical models of Smith and McLean (1977), Wiberg and Smith (1983), and Kachel and Smith (in press). The plots also include any effects of sediment cohesion. Thus it is not surprising that plots from field data (Fig.8) show a different functional relationship than that described by eqn.(4).

Suspended sediment profiles

The observed suspended sediment profiles have been modeled (Fig.9) using three conditions applied to the Rouse equation: (1) C_ϕ, individual sizes 4—11 ϕ and the reference concentration C_a measured at z = 20 cm; (2) C_f, individual sizes 4—6 ϕ, with flocs representing the 7—11 ϕ size range and C_a as measured at z = 20 cm; and (3) C_s, individual sizes 4—6 ϕ, with flocs representing the 7—11 ϕ size range, and C_a as predicted from eqn.(6).

In the computations a sediment-induced stratification correction to the Von Karman constant (eqn.2) has been applied to all three conditions by computing Ri (eqn.3) from the concentration gradient between C_{14} and C_{20}. The corrected value of k' has been substituted in eqn.(1) only for the estimate of C at z = 14 cm. This correction, although minor in its influence

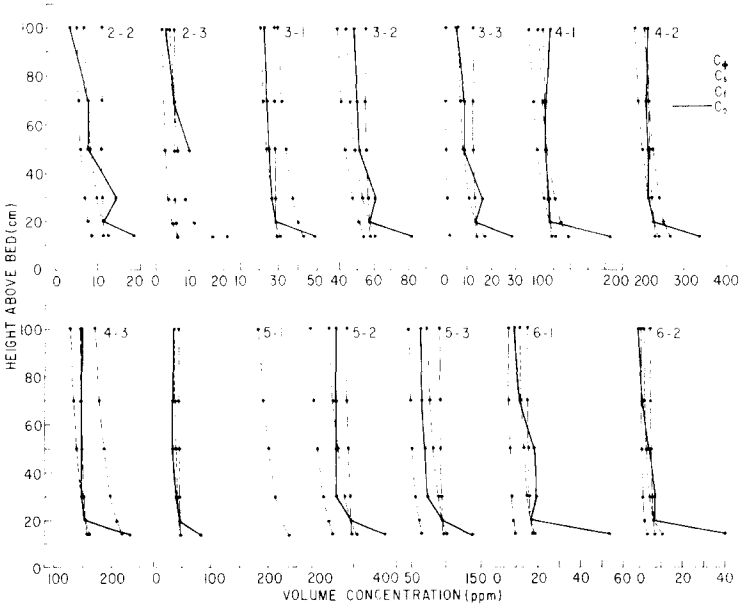

Fig.9. Comparison of modeled (C_ϕ, C_s, C_f) and observed (C_o) concentration profiles for each sampling series.

on the modeled concentration profiles, represents a first approximation in accounting for sediment-induced stratification as suggested by Adams and Weatherly (1981).

The analytical procedure used to model the suspended sediment concentration profiles was to compute C for each phi size or group of phi sizes for the three conditions outlined and at six levels of z (14, 20, 30, 50, 70 and 100 cm). C_ϕ, C_f, and C_s are the sums of concentration values (C) at each level for the appropriate conditions. The resulting profiles for C_ϕ, C_f, and C_s, as well as the observed profile (C_o), are shown in Fig.9 for each of the 13 sampling times.

At levels above 20 cm the comparison between the predicted and observed profiles is relatively good. The predicted profiles of C_ϕ tend to be steeper than the observed profiles (except for profiles 4-1, 4-2 and 4-3), while profiles of C_f more closely follow observed concentration gradients. By arbitrarily varying the values of w_s representing the floc fraction in eqn.(1), the C_f profiles in Fig.9 can be adjusted so that they closely agree with the observed (C_o) profiles. The arbitrary values of w_s that produce close agreement for each profile and their mean value (0.28 cm s^{-1}) that was used for computing the C_f profiles (Fig.9) are listed in Table 1. The profiles of C_s have offsets from the observed curves since they are not forced through the reference level.

At levels below 20 cm the C_o profiles consistently exhibit a sharp increase in concentration toward the seabed (Fig.9). In all cases the modeled profiles did not predict this increase. Possible explanations are: (1) the sediment-induced stratification effects are greater than accounted for; (2) changes in floc structure characterized by substantial variations in w_s; (3) improper characterization of boundary shear stress from velocity profiles (as suggested by the results of Gross and Nowell, 1983); (4) different characterization of the vertical eddy viscosity from that used to derive eqn.(1) (as suggested by Vincent et al., 1982); and (5) eqn.(1) is not sufficient for modeling floc dynamics. Any one or any combination of these factors might account for the inability of the modeling procedures to describe the observed profiles within 20 cm of the seabed.

A direct way to compare the degree to which the modeled profiles describe the observed profiles is by computing a fractional deviation of each modeled value (C_ϕ, C_f, C_s) from its equivalent observed value divided by the observed value:

$$\frac{(C_\phi, C_f, \text{ or } C_s) - C_o}{C_o} \tag{7}$$

A plot of the fractional deviations for C_ϕ, C_f, and C_s versus boundary shear stress (τ_0) is shown in Fig.10. The deviation of C_ϕ (Fig.10A) varies between ± 2.0, and decreases as τ_0 increases. One data value for profile 6-2 is far offscale due to the very low observed concentration at z = 100 cm (Fig.9). Other than this singular value, all data from z = 14, 30, 50, 70, and 100 cm levels are shown. The standard deviation of the data (exclusive of

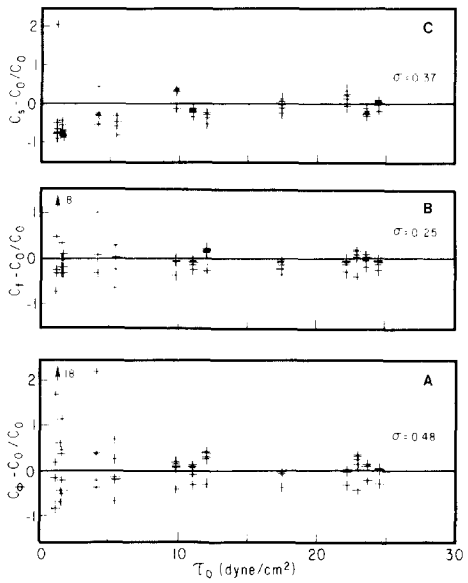

Fig.10. Fractional deviation of each of the modeled concentrations, C_ϕ (A), C_f (B), C_s (C) from the corresponding observed concentrations vs. boundary shear stress. Data from z = 14, 20, 30, 50, 70, and 100 cm are included. The number by the arrow in (A) and (B) refer to an offscale data point. The standard deviation is shown in each figure.

the offscale data point) is ±0.48. The fractional deviation for C_f (Fig.10B) is large at low values of τ_0 and decreases as τ_0 increases. As in Fig.10A one data point (profile 6-2, at 100 cm) is offscale. Disregarding this value the standard deviation of the data is ±0.25. The fractional deviation of C_s (Fig.10C) tends to show a pronounced trend for negative values at low τ_0 to the zero line at τ_0 of approximately 10 dyne cm^{-2}. This trend may indicate some curvature in the data (Fig.8B) but also could be the result of the linear regression analyses which tends to emphasize the higher deviations associated with the higher concentration values so the curve matches the data best at high values of τ_0. The singular data point that falls offscale in Fig.10A and B has a value of 2.0 for C_s. The data from suspended sediment profile 5-1 are not included in Fig.10C because they represent data collected from non-neutral boundary layer conditions. The standard deviation of the C_s data (disregarding the singular point) is ±0.37.

Sensitivity analysis of variables

The major parameters used in eqn.(1) and (6) to model the observed concentration profiles are w_s, U_*, and both the measured and computed values of C_a. A sensitivity analysis was carried out on these parameters to estimate their relative effect on the magnitude of the modeled profiles. The standard deviation or standard error of estimate was determined for w_s-flocs

(Table 1), U_* (from each velocity profile), and C_a (from the data shown in Fig.8B). The floc settling velocity rather than individual particle settling velocities was used for analysis because it was associated with the greatest errors of estimate. The results are expressed as deviations from the means where: w_s-floc = 0.28 ± 0.19 cm s^{-1} (±12%); U_* = 3.21 ± 0.93 cm s^{-1} (±6%); C_a = 82.9 ± 39.9 ppm (±48%). The numbers in parentheses represent the percentage change in C_{100}, when w_s, U_*, and C_a are each varied over the range of the standard deviation or standard error of estimate while holding the other variables at their mean value. These calculations show that the modeled profiles are substantially more sensitive to errors in the estimate of C_a than to those of w_s and U_*; these findings have varying implications in regard to the results of this study. For example, the comparisons of C_ϕ and C_f with C_o (Figs.9 and 10) involves only the slopes of the profiles (they have common values of C_a), thus the deviations in w_s and U_* represent less than a 12% variation in the predicted concentrations. On the other hand, the comparison of C_s with C_o (Figs.9 and 10) involves both differences in profile slopes and profile offsets (the C_s profiles are not forced through C_a), thus errors in measuring or estimating C_a (e.g., eqn.6) lead to greater uncertainties, or a much broader confidence interval, in the prediction of suspended-sediment concentrations.

Mass flux profiles

Estimates have been made of the mass flux of suspended sediment at the times during each tidal series shown in Fig.5. Comparison of flux profiles from the field measurements and those from the predicted concentration profiles are shown in Fig.11. The measured flux profiles are the product of the observed concentration and speed at z = 14, 20, 30, 50, 70 and 100 cm,

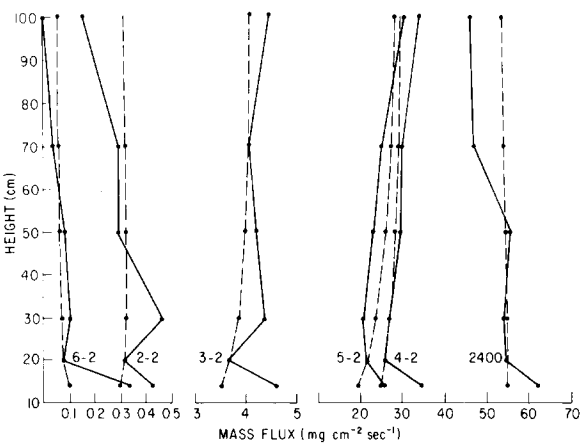

Fig.11. Measured (solid line) and predicted (dashed line) profiles of mass flux at times of concentration profiles shown in Fig.5. Note scale change on the abscissa.

respectively. Speed estimates at z = 15 and 30 cm were made by log-linear extrapolation from adjacent levels. The predicted flux profiles are the product of the predicted concentration profiles of C_f (Fig.9) and the slope of the velocity profile with the mass flux at z = 20 cm set as the reference level.

Above z = 20 cm the magnitude of the horizontal flux is relatively uniform, exhibiting only minor variations with distance above the bed. The mass flux during low-transport conditions (e.g., series 2-2, 6-2) tends to decrease slightly with increasing elevation while during higher-transport conditions (e.g., series 3-2, 4-2, 5-2) the magnitude of the mass flux increases slightly away from the seabed. These minor variations in the vertical are the result of differences in the balance between the velocity and concentration profiles. During low-transport conditions the decrease in suspended sediment concentration away from the bed is pronounced and causes the mass flux profile to decrease accordingly. During high-transport conditions the concentration profiles are more uniform vertically and the increased velocity away from bed tends to make the mass flux profiles increase slightly with distance from the seabed.

Below z = 20 cm the magnitude of the mass flux increases sharply towards the seabed (Fig.11), reflecting the high suspended sediment concentration gradient observed in all profiles (Fig.9). Neither the predicted concentration profiles nor the predicted mass flux profiles show this increase.

SUMMARY

Time-series measurements of suspended sediment and velocity profiles within 1 m of the seabed have been used to test the ability of the suspended sediment distribution equation to predict near-bottom suspended sediment distributions in a tidal channel in San Francisco Bay, California. Based on these evaluations the following results were obtained:

(1) Using eqn.(1) with a simplified sediment-induced stratification correction and measured values of the reference concentration at z = 20 cm predicted suspended sediment concentrations are within approximately ±50% of the measured values.

(2) Analysis of the particle-size distribution of the suspended load for various flow conditions suggests that the 4—6 ϕ sized particles tend to respond independently to variations in boundary shear stress, while the 7—11 ϕ sized particles tend to respond as an assemblage. One possible explanation for this constancy of size distributions regardless of particle concentrations is that the 7—11 ϕ particles occur as flocs. Using a floc settling velocity of 0.28 cm s^{-1} and critical shear stress of 0.49 dyne cm^{-2} in eqn.(1) predicted values of suspended sediment concentrations are within approximately ±25% of the measured values.

(3) An empirical relationship for estimating the reference concentration (C_a) as a function of the bed concentration ($i_b C_b$) and excess shear stress (S) is:

$$C_a = i_b C_b \ (2.53 \times 10^{-7} \ s^2 + 3.63 \times 10^{-6}) \qquad (6)$$

Using estimations of C_a from eqn.(6) in eqn.(1), predicted values of the suspended sediment concentrations are within approximately ±40% of the measured values.

(4) A sensitivity analysis of the variables w_s, U_*, and C_a showed that eqn.(1) is about four times more sensitive to variations in estimates of C_a than for w_s or U_*. For example, varying w_s or U_* in eqn.(1) by its standard deviation changes the predicted value of C_{100} by ±12% or less. Varying C_a by its standard deviation changes C_{100} by ±48%.

(5) The mass flux of suspended sediment is approximately uniform between $z = 20$ and 100 cm. Below $z = 20$ cm the mass flux increases sharply reflecting an increase in suspended sediment concentration that was also observed.

ACKNOWLEDGMENTS

The authors wish to acknowledge R. Johnson and T. Milligan for their assistance in the field, T. Milligan for the textural analysis of the suspended sediment samples, and A. Nowell and D. Henry for critical review of the manuscript. This research was carried out under NSF Grant No. OCE 81-11500. Contribution No. 1617, School of Oceanography, University of Washington, Seattle, Wash.

REFERENCES

Adams, C.E. and Weatherly, G.L., 1981. Suspended-sediment transport and benthic boundary-layer dynamics. Mar. Geol., 42: 1—18.

Cacchione, D.A. and Drake, D.E., 1979. Sediment transport in Norton Sound, Alaska: Regional patterns and geoprobe system measurements. U.S. Dep. of Interior, Geol. Surv., Open File Rep. 79-1555, 88 pp.

Dietrich, W.A., 1982. Settling velocity of natural particles. Water Resour. Res., 18: 1615—1626.

Drake, D.E. and Cacchione, D.A., in press. Estimates of the reference concentration (C_a) and resuspension coefficient (γ_0) from near-bottom observations on the California shelf. Cont. Shelf Res.

Einstein, H.A. and Chien, N., 1952. Second approximation to the solution of the suspended load theory. Inst. Eng. Res. and U.S. Army Corps of Engineers, Missouri River Div., M.R.D. Sediment Ser. No. 3, 30 pp.

Einstein, H.A. and Chien, N., 1955. Effects of heavy sediment concentration near the bed on velocity and sediment distribution. Inst. Eng. Res. and U.S. Army Corps of Engineers, Missouri River Division, M.R.D. Sediment Ser. No. 8, 76 pp.

Glenn, S.M., 1983. A continental shelf bottom boundary layer model: The effects of waves, currents, and a movable bed. Diss. Woods Hole Oceanographic Institution, Woods Hole, Mass., 237 pp.

Gross, T.F. and Nowell, A.R.M., 1983. Mean flow and turbulence scaling in a tidal boundary layer. Cont. Shelf Res., 2: 109—126.

Heathershaw, A.D., 1979. The turbulent structure of the bottom boundary layer in a tidal current. Geophys. J.R. Astron. Soc., 58: 395—430.

Hsia, C.H., 1943. A study of transportation of fine sediments by flowing water. Ph.D. Diss., State Univ. of Iowa, Ames, Iowa.

Kachel, N.B. and Smith, J.D., in press. Geologic impact of sediment transporting events on the Washington continental shelf. In: J.R. Knight (Editor), Shelf Sands and Sandstones Symposium June 1984. Can. Assoc. Pet. Geol. Calgary, Alta.

Komar, P.D., 1978. Boundary layer flow under steady unidirectional currents. In: D.J. Stanley and D.J.P. Swift (Editors), Marine Sediment Transport and Environmental Management. Wiley-Interscience, New York, N.Y., pp.91—125.

Kranck, K., 1980. Experiments on the significance of flocs in the settling of fine grain sediment in still water. Can. J. Earth Sci., 17: 1517—1526.

Kranck, K. and Milligan, T., 1979. The use of the Coulter Counter in Studies of particle-size-distributions in aquatic environments. Bedford Inst. of Oceanography, Rep. Ser. B1-R-79-7, 48 pp.

Kranck, K. and Milligan, T., 1980. Macroflocs: Production of marine snow in the laboratory. Mar. Ecol. Prog. Ser., 3: 19—24.

Krone, R.B., 1972. A field study of flocculation as a factor in estuarine shoaling processes. Committee on Tidal Hydraulics, U.S. Army Corps of Engineers, Waterways Experimental Station, Vicksburg, Miss., Tech. Bull. 19.

Lane, E.W. and Kalinski, A.A., 1939. The relation of suspended to bed material in rivers. Trans. Am. Geophys. Union, 20: 637—641.

McCave, I.N., 1973. Some boundary-layer characteristics of tidal currents bearing sand in suspension. Mem. Soc. R. Sci. Liège, 6: 107—126.

Miller, M.C., McCave, I.N. and Komar, P.D., 1977. Threshold of sediment motion under unidirectional currents. Sedimentology, 24: 507—527.

Nowell, A.R.M., Jumars, P.A. and Eckman, J.E., 1981. Effects of biological activity on the entrainment of marine sediments. Mar. Geol., 42: 133—172.

Pien, C.-L., 1941. Investigation of turbulence and suspended material transportation in open channels. Ph.D. Diss., State Univ. of Iowa, Ames, Iowa.

Rouse, H., 1937. Modern conceptions of the mechanics of fluid turbulence. Trans. Am. Soc. Civ. Eng., 102: 463—554.

Shi, N.C., Larsen, L.H. and Downing, J.P., 1985. Predicting suspended sediment concentration on continental shelves. Mar. Geol., 62: 255—276.

Smith, J.D., 1977. Modeling of sediment transport on continental shelves. In: E.D. Goldberg et al. (Editors), The Sea, 6, Wiley, New York, N.Y., pp.539—577.

Smith, J.D. and McLean, S.R., 1977. Spatially averaged flow over a wavy surface. J. Geophys. Res., 82: 1735—1746.

Sternberg, R.W., Johnson II, R.V., Cacchione, D.A. and Drake, D.E., 1986. An instrument system for monitoring and sampling suspended sediment in the benthic boundary layer. Mar. Geol., 71: 187—199 (this volume).

Sundborg, A., 1956. The river Klaralven: A study of fluvial processes. Medd. Uppsala. Univ. Geogr. Inst., Ser. A., No. 115, pp.127—316.

Task Committee on Preparation of Sedimentation Manual, 1963. Sediment transportation mechanics: Suspension of sediment. J. Hydraul. Div., Am. Soc. Civ. Eng., 89 (HY5): 45—76.

Vanoni, V.A., 1953. Some effects of suspended sediment on flow characteristics. State Univ. Iowa, Ames, Iowa, Bull. No. 34, pp.137—158.

Vincent, C.E., Young, R.A. and Swift, D.J.P., 1982. On the relationship between bedload and suspended sand transport on the inner shelf, Long Island, New York. J. Geophys. Res., 87: 4163—4170.

Wiberg, P. and Smith, J.D., 1983. A comparison of field data and theoretical models for wave—current interactions at the bed on the continental shelf. Cont. Shelf. Res., 2: 147—162.